Available online at www.sciencedirect.com
ScienceDirect
Journal of the European Ceramic Society 30 (2010) 1629–1640
www.elsevier.com/locate/jeurceramsoc

Mechanisms and orientation dependence of the corrosion of single crystal Cordierite by model diesel particulate ashes

Nicolas Maier [a,b], Klaus G. Nickel [b,*], Christine Engel [a], Andreas Mattern [a]

[a] *Robert Bosch GmbH, CR/ARM2, Postfach 10 60 50, D-70049 Stuttgart, Germany*
[b] *University Tübingen, Applied Mineralogy, Wilhelmstr. 56, D-72074 Tübingen, Germany*

Received 15 September 2009; received in revised form 21 December 2009; accepted 10 January 2010
Available online 1 February 2010

Abstract

Cordierite $Mg_2Al_4Si_5O_{18}$ is a material for diesel particulate filters (DPF) with high potential. Its resistance to two simplified model ashes has been tested on single crystals at temperatures up to 1050 °C, which are realistic for use under 'worst case' conditions. Single crystals were examined in order to investigate the orientation dependence of attack due to the strongly anisotropic nature of the Cordierite crystal lattice. A mixture of sodium carbonate and silica was used to study the attack of an alkali-rich ash composition and a mixture of the Ca, Mg and Zn orthophosphates to study an ash composed of typical main constituents of ashes found in DPF used in traffic. The sodium-rich ash formed a melt and attacked the Cordierite by dissolving it. No anisotropy in the corrosion was observed, because the attack is controlled by outward diffusion of Mg. A kinetic break occurs in the system, caused by the formation of a Nepheline product layer, slowing down corrosion. A much stronger corrosion of Cordierite occurs by the phosphate mixture at 1050 °C. Excessive melt formation from the ash causes fast dissolution of the substrate with melt saturation within minutes. Anisotropy of the dissolution process could not be detected. The initial kinetics is dominated by saturation effects, which slow down corrosion. The saturated melt attacks Cordierite by reaction processes leading to the formation of new crystalline phases. This process is much slower than the initial dissolution process but may significantly contribute to the destruction of Cordierite substrates if large contact areas between ash melt and Cordierite exist. Additionally, the formation and local growth of crystalline phases causes the extension of faults, which may eventually become critical.

Keywords: Cordierite; Corrosion; Diesel particulate filter; Electron microscopy; Spectroscopy

1. Introduction

Cordierite $Mg_2Al_4Si_5O_{18}$ has received much attention during the past decades as a potential material for the application in diesel particulate filters (DPF), mainly because of its excellent thermal shock resistance resulting from its very low thermal expansion.[1,2] The corrosion resistance of Cordierite remains an important issue in studies on Cordierite as a material for particulate filters. During use, a DPF collects soot, i.e. carbon-based particles from diesel combustion, as well as small amounts of components other than carbon and organic matter. These typically include compounds containing Ca, Mg, Zn, P and S originating from fuel or lubricating oil, as well as metals or metal oxides from wear of the engine or the exhaust gas system.[3–11] When the soot is periodically burnt off to clean the filter in a so-called "regeneration" process, these components form the so-called "ash", which remains within the filter. If a regeneration process is not well controlled, there is a possibility that very high temperatures above 1000 °C might occur within the filter.[5,12] Even peak temperatures exceeding 1100 °C have been reported.[13,14] At these high temperatures, the ash may damage the Cordierite filter material. Possible deterioration mechanisms include reactions between ash and Cordierite[4–6,15–20] or melting of the Cordierite below its intrinsic melting point by the formation of eutectic liquids between ash and filter material.[3,5,17–19,21] Reaction products and critical temperatures for the attack of numerous potential ash compositions (single components or component mixtures) on Cordierite DPF have been reported in the literature cited above. However, information on actual processes occurring during the corrosion of Cordierite by ashes, which determine the progress and velocity of the corrosion, is scarce.

* Corresponding author. Tel.: +49 7071 29 76802; fax: +49 7071 29 3060.
E-mail address: klaus.nickel@uni-tuebingen.de (K.G. Nickel).

0955-2219/$ – see front matter © 2010 Elsevier Ltd. All rights reserved.
doi:10.1016/j.jeurceramsoc.2010.01.018

Various studies have shown that compounds of alkaline elements Na and K are particularly critical in respect to a corrosive degradation of Cordierite substrates.[6,15,17,18,20,22] Alkaline compounds can be accumulated in ashes from de-icing salt on roads during winter or from salt-rich air in seaside areas.[8] Alkaline compounds might also be introduced by catalytic coatings applied to DPF in order to combine filter function with catalytic properties.[23] Sodium compounds have also been suggested as fuel-borne catalysts to reduce filter regeneration temperatures[24]; when such catalysts are used, high sodium concentrations in ashes have to be expected as catalysts strongly contribute to ash formation. Finally, contents of alkaline elements from biodiesel fuel blends[25] or accidentally contaminated diesel fuels might contribute to ash.

Two slightly different crystal structures of Cordierite, a hexagonal "high temperature" form (Indialite) and an orthorhombic "low temperature" form, are known.[26,27] Most natural and synthetic Cordierites do not belong to a pure modification, but a mixed structure between the two end members.[26,27] Both modifications have a strongly anisotropic crystal structure with large channel-like structures in the direction of one crystallographic axis (further referred to as the c_0-axis, as it corresponds to the c_0-axis in the hexagonal modification and also in the orthorhombic modification, provided that the allocation of the crystallographic axes is chosen so that $a_0 > b_0 > c_0$).

Based on experimental observations and literature reports, Montanaro et al. raised the question whether these channel structures have an influence on the corrosion of Cordierite as the diffusion of ions in channels might increase the amount or velocity of the deterioration of Cordierite.[12,20] However, a study by Bachiorrini[28] aimed at answering this question via measurements with IR spectroscopy on reacted mixtures of Cordierite and sodium carbonate showed no evidence for the diffusion of sodium in the Cordierites channel structures. Therefore, the channel structures do not provide a pathway for significantly enhanced diffusion of alkali atoms in the Cordierite structure during corrosive attack. However, the strongly anisotropic crystal lattice still makes significant differences in the corrosion resistance of the material in different crystal directions likely. Such differences may be very important for the degradation behavior of typical Cordierite DPF, which are made from extruded honeycombs. In these extruded bodies, a strong orientation of Cordierite crystals exists.[1,2] Therefore, anisotropy in the corrosion resistance of the Cordierite lattice might strongly influence the deterioration process of the filter material during attack by ashes.

In this paper we present results of a study on the attack of ashes on natural single crystals and give models to provide new insight in deterioration processes of Cordierite DPF during ash attack.

2. Experimental

Experiments were performed on samples from a natural Cordierite single crystal from the Republic of South Africa. Chemical composition as determined by inductively coupled plasma optical emission spectroscopy with carrier gas hot extraction for the determination of carbon content is given in Table 1.

Table 1
Chemical composition of Cordierite crystal.

Oxide	Content (wt%)
Al_2O_3	33.7
MgO	11.8
SiO_2	48.0
Fe_2O_3	3.03
MnO	0.22
Na_2O	0.33
CO_2	0.43

The orientation of the crystallographic c_0-axis within the crystal, corresponding to the direction of the channel structures in the Cordierite lattice, was identified by XRD. Subsequently, samples with surfaces orientated perpendicular and parallel to the axis c_0, respectively, were cut out of the crystal. Sample surfaces were ground with a 500-grit abrasive paper to ensure equal surface roughness in all cases.

For corrosion experiments, pellets with a diameter of 8 mm were pressed from 0.1 g of ash and placed on the sample surfaces. Two different ash compositions were used:

(1) A mixture of 1 mole of Na_2CO_3 with 1.5 moles of SiO_2 (*sodium silicate ash*). The mixture was used to examine the corrosion of Cordierite in a very alkali-rich environment. This mixture reacts to sodium silicate(s) and gaseous CO_2 at high temperatures.[29,30] The phase diagram[31] indicates an onset of melting at 830 °C and complete melting at app. 930 °C for the chosen ratio of Na_2O to SiO_2. From literature reports as mentioned in Section 1, it is known that sodium compounds like Na_2CO_3 cause severe corrosion already at temperatures several hundred degrees below 1000 °C if atmospheric conditions allow for the formation of highly reactive Na_2O. According to reports on the composition of ashes collected from DPF,[3,9,11,32] sodium occurs only as a minor component in many ashes. However, if high sodium levels are accumulated in a filter from one or more of the sources mentioned in Section 1 or if low-melting alkaline compounds segregate from an ash as melts and thus get concentrated on filter surfaces, sodium attack on DPF substrates is likely to play a crucial role in filter degradation. The formation of sodium-rich melts is known from corrosion experiments of Cordierite with pure sodium salts.[17,18] Therefore, alkali attack on Cordierite through an alkali-rich melt is expected during worst case regenerations of DPF if the filter is in contact with alkali-rich ash. The mechanisms of the corrosion of Cordierite by such melts have never been examined in detail yet. The model ash used is likely to represent a corrosion process as it may occur after some initial reaction between Cordierite and high alkali ashes; initial reactions between Cordierite and pure sodium compounds, which may occur at temperatures even lower than reactions between Cordierite and the ash composition used here, cannot be examined in experiments with the sodium silicate

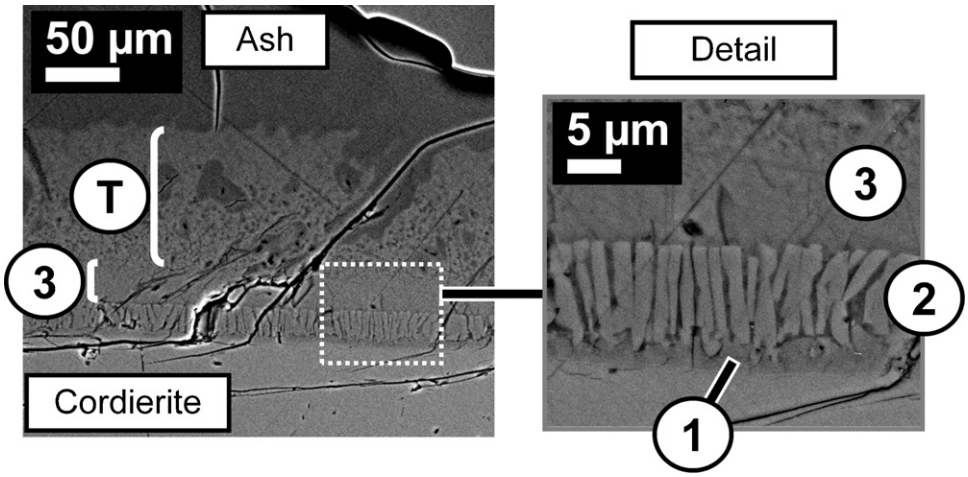

Fig. 1. SEM image (cross-section) of the interface between Cordierite and sodium silicate ash after 5 min at 1000 °C; numbers 1...3 indicate corrosion zones; T = transition zone.

ash. The attack of alkali-silicate melts on filter substrates might also occur as a genuine corrosion process if an ash contains high amounts of silica (which might originate from dust particles in the inlet air[9,11] or be leached from engine sealing components[33]) additional to alkali compounds.

(2) An equimolar mixture of $Ca_3(PO_4)_2$, $Mg_3(PO_4)_2$ and $Zn_3(PO_4)_2$ (*phosphate ash*). Orthophosphates of Ca, Mg and Zn are typical main constituents of real filter ashes according to literature,[3,9–11] so the corrosion mechanism by the attack of these phosphates is expected to be highly relevant for the deterioration of Cordierite filters in realistic environments.

The Cordierite samples with the ash pellets were placed in covered alumina crucibles and exposed to isothermal heat-treatments with different maximum temperatures and exposure times in a tube furnace. Heating and cooling rates were 250 °C/h in all tests.

Pellets with the sodium silicate ash were heat-treated at 1000 °C for 5, 30 and 60 min to examine the development of corrosion at a 'worst case' regeneration temperature of a DPF. An additional test was made with 5 min exposure time at 900 °C to examine the ash attack under less severe conditions.

Pellets with the phosphate ash were heat-treated at 1000 °C for 30 min in a first test. No corrosive attack was visible after this treatment, thus further experiments were performed at 1050 °C with exposure times of 10 and 20 min. This temperature is less likely to occur within a filter than the 1000 °C chosen for the tests with the sodium silicate ash, but it is still well within the range of possible temperatures reported for 'worst case' filter regenerations.[13,14] Cross-sections of the corroded samples were prepared by embedding the samples in a resin, followed by grinding and polishing.

The cross-sections were examined with scanning electron microscopy (SEM) and energy dispersive X-ray spectroscopy (EDX) using a LEO *35VP* microscope with an OXFORD *INCA x-sight* EDX detector. Micro-X-ray diffraction (XRD) was used to identify crystalline phases in cross-sections of corroded samples using a BRUKER D8 Advance microdiffractometer (Bruker-AXS GmbH, Karlsruhe, Germany) with CoKα radiation and a HOPG graphite primary monochromator. The diffractometer is equipped with an areal detector. CuKα radiation was used. The irradiated spot size was below 100 µm.

Additional XRD examinations were performed on a powder mixture of phosphate ash and Cordierite (ratio 4:1 on a molar basis) after 10 min heat-treatment at 1050 °C for additional information on reaction products. A BRUKER-AXS *D8* diffractometer (CuKα radiation, Bragg-Brentano optics, scintillation counter) was used for the measurement. Element distributions in cross-sections of corroded samples were additionally analyzed by time-of-flight secondary ion mass spectrometry (TOF-SIMS) using an IonTOF *IV* spectrometer. Areas of approximately 200 µm × 200 µm were analyzed. Primary ions were Bi^+ (energy: 25 keV). The lateral resolution was approximately 500 nm.

3. Results

3.1. Samples with sodium silicate ash

Ash pellets were strongly deformed after all heat-treatments. Their appearance was glassy, indicating strong melt formation during the heat-treatments.

After all treatments at 1000 °C, a typical damage pattern was found. Above a remaining unreacted Cordierite, several zones, differing in their element contents (as measured by EDX and confirmed by TOF-SIMS) were found. In Fig. 1, this pattern is shown for a sample after 5 min corrosion at 1000 °C. Element contents of the respective corrosion zones as measured by EDX are depicted in Fig. 2. The following corrosion zones were identified:

(1) "Zone 1" has a ratio Na/Si in the range between 0.7 and 1.0, an Al content of 10–12 at.% and 1–2 at.% Mg. Crystal-shaped features were sometimes observed.

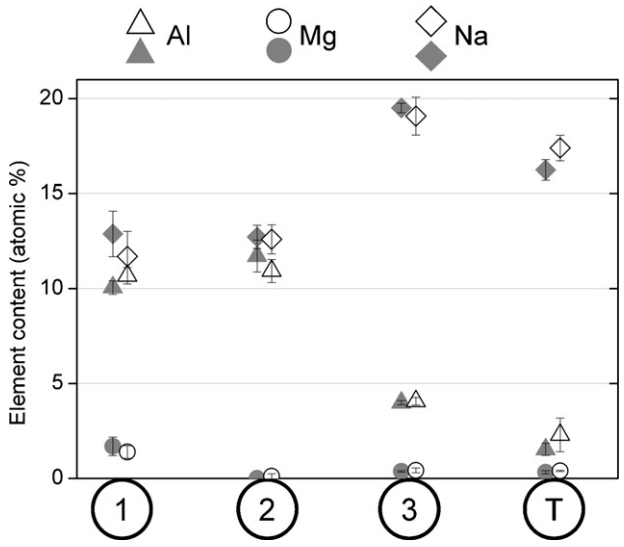

Fig. 2. Element contents of corrosion zones as measured by EDX in samples after 5 min corrosion at 1000 °C with sodium silicate ash; numbers 1...3 indicate corrosion zones; T = transition zone; filled symbols: ash on surface perpendicular to c_0; open symbols: ash on surface parallel to c_0; error bars indicate standard deviations.

(2) "Zone 2" has a well-defined ratio Na/Si in the range between 0.8 and 0.9. The Al content is comparable to zone 1, the Mg content certainly much lower than in zone 1. Often, no magnesium was detected at all in EDX measurements. The zone appears to consist of lath-shaped oriented crystals mainly. Micro-XRD measurements, which showed no crystalline phases within the ash bulk after corrosion, identified the presence of Nepheline $NaAlSiO_4$ near the interface between Cordierite and ash (see Fig. 3). Therefore zone 2 is taken to consist mainly of Nepheline.
(3) "Zone 3" is chemically distinct with a much lower Al content of app. 4 at.% only. The Na content is much higher than in zones 1 and 2, the ratio Na/Si lies between 0.9 and 1.1 and is thus comparable to zone 1. The Mg content is lower than in zone 1, but higher than in zone 2.
(4) Above zone 3, with or without a transition zone, we have the ash bulk. In all samples, the ratio Mg/Al is >0.5. This is a higher Mg/Al ratio than the Cordierite substrate. Carbon contents within the ash are close to or below the detection limit of EDX, i.e. ≪1 at.%.

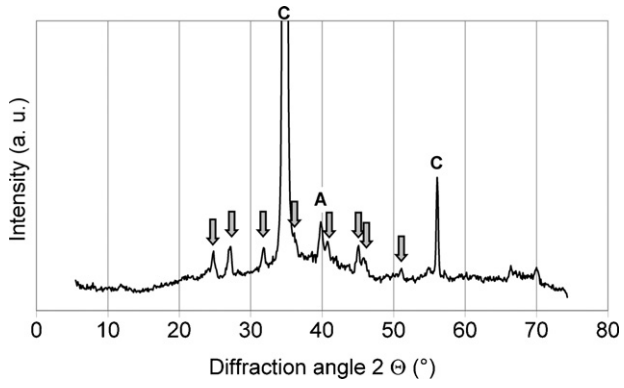

Fig. 3. XRD pattern of corrosion products near the interface Cordierite–ash after 1 h corrosion at 1000 °C with sodium silicate ash; arrows mark reflexes from Nepheline; "C" marks reflexes from Cordierite; "A" marks an artifact signal from the X-ray optics.

The distinct transition zone between zone 3 and the ash bulk ("T" in Fig. 1) present after 5 min heat-treatment at 1000 °C is characterized by low contents of Al (<3 at.%) and Mg (<0.5 at.%) and becomes fuzzy for longer exposure times at 1000 °C.

With increasing exposure time, no distinct development of the compositions of the corrosion zones was detectable. The compositions stay constant within the error limits (standard deviations of measured average values) or show only slight irregular uncorrelated variations. This is depicted in Fig. 4 for the development of Al, Mg and Na contents of zones 1 and 3 with increasing time at 1000 °C.

However, the thickness of the corrosion zones 1 and 2 clearly increases with time (Fig. 5). A linear fit of the growth of the zones during dwell time at 1000 °C gives a growth rate of 0.090 μm/min with an intercept of 2.9 μm for zone 1 ($R^2 = 0.9997$), and a growth rate of 0.044 μm/min with an inter-

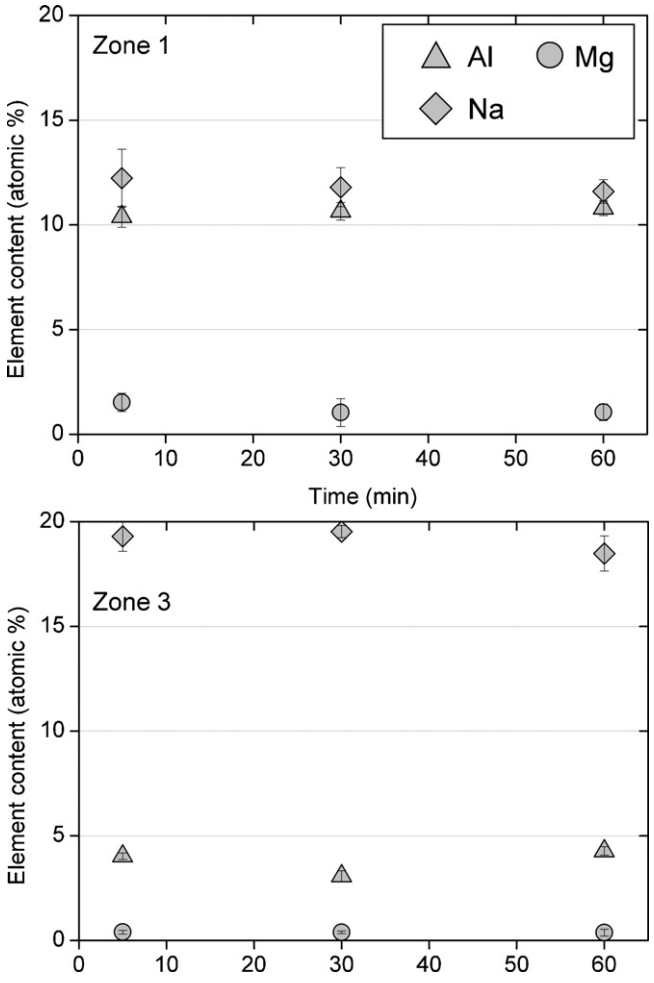

Fig. 4. Development of Al, Mg and Na contents of corrosion zones 1 and 3 during corrosion with sodium silicate ash at 1000 °C as measured by EDX; average values for samples with ash orientated parallel and perpendicular to c_0; error bars indicate standard deviations.

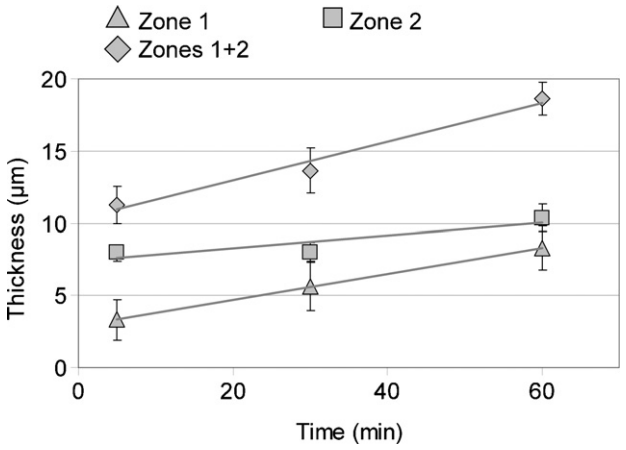

Fig. 5. Development of the thickness of corrosion zones 1 and 2 during corrosion with sodium silicate ash at 1000 °C; average values for samples with ash orientated parallel and perpendicular to c_0; error bars indicate standard deviations.

cept of 7.4 μm for zone 2 ($R^2 = 0.80$). The combined growth rate for zones 1 and 2 is 0.135 μm/min with an intercept of 10.2 μm ($R^2 = 0.98$). Thus zone 1 seems to develop much faster than zone 2.

Information on the possible growth of zone 3 could not be deduced due to the increasingly fuzzy transition between zone 3 and the ash bulk with increasing exposure time.

In the sample heat-treated for 5 min at 900 °C, no individual corrosion zones could be resolved. In SEM images, an overall zone with a thickness of <5 μm can be distinguished within the ash directly at the interface between ash and Cordierite. In EDX measurements, this zone showed significantly higher Al contents and lower Mg contents than the ash directly above this zone (see Fig. 6).

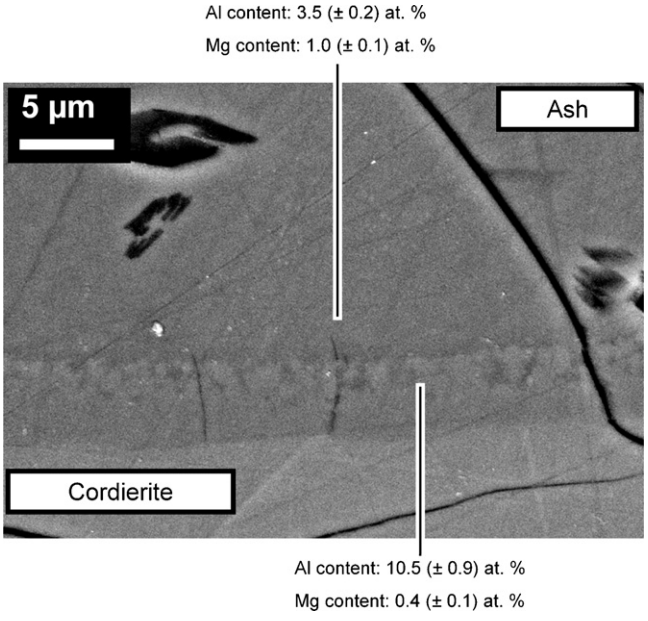

Fig. 6. SEM image (cross-section) of the interface Cordierite–ash after 5 min corrosion at 900 °C with sodium silicate ash; element contents of two different zones within the ash as measured by EDX.

No evidence for any diffusion of sodium into the Cordierite was found. In EDX measurements as well as in TOF-SIMS measurements, a distinct step-like pattern was measured for the sodium content at the interface between ash and Cordierite without any increase of Na content within the Cordierite near the interface. This result was obtained for both orientations of ash relative to Cordierite.

No significant differences in the element contents of the corrosion zones (i.e. differences without overlap of the standard deviations of measured average values) were detected for samples with different orientations of ash relative to the Cordierite lattice. Thus, surprisingly, the distinct anisotropy of the structure of Cordierite is not reflected in the corrosion behavior.

3.2. Samples with phosphate ash

3.2.1. Powder mixture

XRD measurements on the powder mixture of Cordierite and phosphate ash after 10 min at 1050 °C showed a complex pattern indicating the presence of numerous different phases. In accordance with the EDX measurements on the corroded crystals (see below), the following phases could be identified:

(1) A phase with Stanfieldite ($Ca_4(Mg,Zn)_5(PO_4)_6$) structure.
(2) Silica in the form of Cristobalite.
(3) A spinel phase with zinc-rich composition.

Several main reflexes in the diffractogram could not be assigned to any phase included in the International Center for Diffraction Data's *PDF4+* database. It is assumed that these reflexes belong to a Ca–Mg–Zn phosphate phase as identified by EDX measurements (see below). No increased background is present in the diffractogram, indicating that contents of amorphous phases in the ash after heat-treatment are low. Only weak signals from Cordierite were identified, indicating that a large fraction of the Cordierite in the powder mixture has been converted to other phases.

3.2.2. Single crystal–ash pairs

After 30 min heat-treatment at 1000 °C, strong sintering of the ash (shrinkage of the ash pellet and low porosity within the pellet after heat-treatment) was observed. Results of SEM and EDX measurements on a cross-section through heat-treated sample indicate the formation of mixed Ca–Mg–Zn phosphates within the ash. However, no indications for any interaction between Cordierite and ash were observed.

After 10 min at 1050 °C, the ash pellet appeared strongly deformed, indicating excessive melt formation. In SEM and EDX examinations, considerable corrosive attack of the ash on the Cordierite was evident. The surface of the Cordierite below the ash has receded irregularly up to several tens of micrometers relative to the original surface as extrapolated from uncorroded areas of the Cordierite adjacent to the corroded areas below the ash pellet. Due to the irregular nature of the Cordierite recession, no reasonable quantification of the depth of this recession was possible.

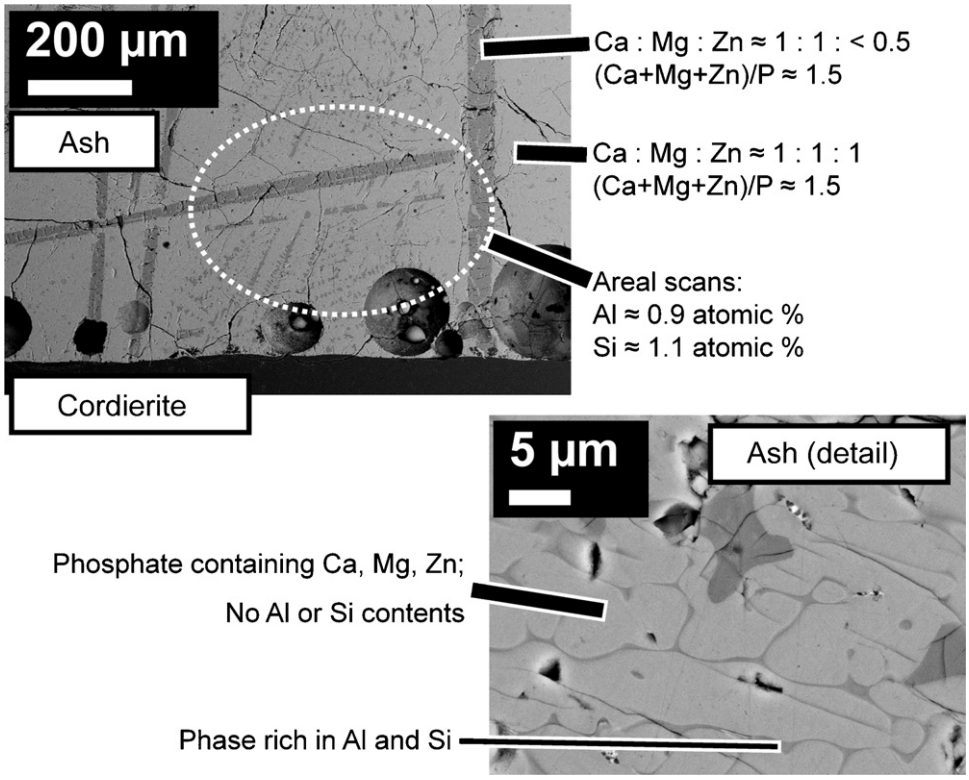

Fig. 7. SEM image (cross-section) of Cordierite and phosphate ash after 10 min at 1050 °C; phase compositions and contents of Al and Si within the ash as measured by EDX.

In the ash above the Cordierite, no distinct zones of different element compositions as in the samples corroded by sodium silicate ash exist. Instead, the ash contains a mixture of several distinguishable phases throughout the whole volume. EDX measurements revealed two different phases rich in phosphorous as the main constituents of the reacted ash (see Fig. 7). One phase contains approximately equal amounts of Ca, Mg and Zn (with slight Zn enrichment); the other phase containing approximately equal amounts of Ca and Mg and clearly lower contents of Zn is probably the Stanfieldite phase identified by XRD in powder experiments. Both phases show ratios (Ca + Mg + Zn)/P of approximately 1.5 in accordance with the composition of $(Ca,Mg,Zn)_3(PO_4)_2$ orthophosphates contained in the original ash.

On a macroscopic scale the distribution of Al and Si in the whole volume of the ash above the Cordierite as measured by EDX areal scans is homogeneous (Fig. 7) and no indications for any diffusion profile were found by EDX or TOF-SIMS. However, locally the distribution of Al and Si within the reacted ash is not homogeneous: SEM and EDX examinations showed that the phosphorous-rich phases which are the main constituents of the ash do not contain any significant amounts of Al or Si. Instead a phase rich in Al and Si appears to form a boundary phase, separating individual grains of the phosphorous-rich phase, which in turn is a homogeneous Ca, Mg and Zn phosphate phase (Fig. 7). The small size of the grain-boundary phase excluded the determination of its exact composition by EDX.

Minor phases detected by EDX throughout the reacted ash showed silica and zinc-rich spinel ($\approx ZnAl_2O_4$) compositions in accordance with XRD measurements on the reacted powder mixture. Large clusters of these phases are found typically near the ash/Cordierite interface (Fig. 8). These clusters are often connected to cracks in the Cordierite: they fill the cracks and reach into the ash as an extension of the cracks. Most probably, these "extensions" of the cracks are formed when Cordierite around a crack filled by the respective phases is removed by corrosion. Phosphorous-rich constituents of the ash in contact with the silica/spinel clusters are generally of the zinc-depleted type (Stanfieldite) (Fig. 8).

No evidence for anisotropic corrosion was found by comparing the Al and Si contents measured by EDX areal scans of the ash in samples with ash deposited on surfaces parallel or perpendicular to the axis c_0 (Fig. 9) and no indications for any diffusion of ash elements into the Cordierite lattice were found by EDX or TOF-SIMS.

4. Discussion

4.1. Samples with sodium silicate ash

The lack of carbon within the ash after the heat-treatments and the molten appearance of the heat-treated ash pellets indicate that the expected formation of a sodium silicate melt from the ash did indeed take place during heat-treatments.

The lack of any indications for a diffusion of sodium into the Cordierite lattice confirms the results of the spectroscopic examinations by Bachiorrini[28] and falsifies earlier hypotheses:[12,20]

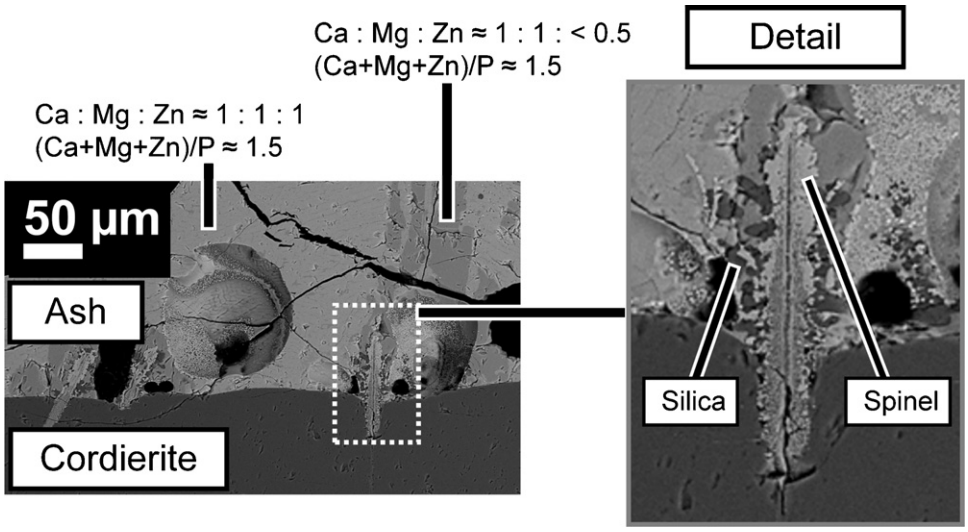

Fig. 8. SEM image (cross-section) of the interface between Cordierite and phosphate ash after 10 min at 1050 °C; phase compositions as measured by EDX.

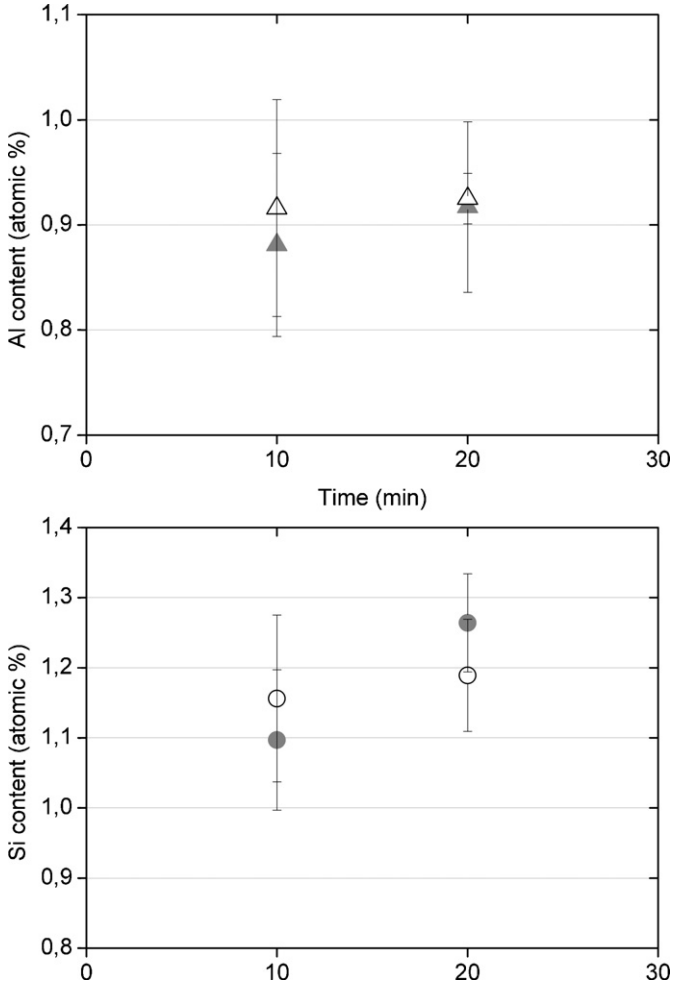

Fig. 9. Al and Si contents of phosphate ash as measured by EDX (areal scans) after 10 and 20 min corrosion time; filled symbols: ash on surface perpendicular to c_0; open symbols: ash on surface parallel to c_0; error bars indicate standard deviations.

The attack of sodium compounds on Cordierite is a surface process.

The following model (Fig. 10) was developed to explain the observed behavior:

1. During heating-up, sodium carbonate reacts with silica to form sodium silicate and gaseous CO_2. In accordance with the phase diagram[31] the sodium silicate forms a melt at temperatures above 830 °C. The sodium silicate melt attacks the Cordierite by dissolving it, hereby enriching the melt in both Mg and Al. The dissolved elements from the Cordierite diffuse away from the ash/Cordierite interface.
2. Mg diffusion is faster than Al diffusion in the melt. This causes the development of a compositional profile within the melt: Al enrichment and high Al/Mg ratios in the ash melt near the Cordierite and low Al/Mg ratios within the ash bulk.
3. After a critical enrichment in Al and a sufficient depletion in Mg in the melt are reached, the crystallization of Nepheline $NaAlSiO_4$ near the ash/Cordierite interface takes place. This Nepheline corresponds to corrosion zone 2 in Fig. 1. The grain boundary phase visible between the crystals has to be rich in silicon and sodium, because the Na content of the zone is slightly higher than the Al content (Fig. 4) and the Na/Si ratio lies slightly below 1.

   The initial formation of a several micrometers thick Nepheline layer after 5 min at 1000 °C and the slow growth afterwards suggest that Nepheline nucleation is crucial for the kinetics of the process. At 900 °C (Fig. 6) the critical condition for Nepheline crystallization seems not to be reached in a short time. Nepheline formation therefore occurs only after a wider distribution of Al and Mg within the ash layer, the crystallization occurring simultaneously within a layer of several micrometers thickness and not as a continuous growth process starting from a thin initial layer.
4. Once a Nepheline layer is established, it acts as a barrier for further diffusion of Mg from dissolved Cordierite into the ash. Mg diffusion is confined to the grain boundaries

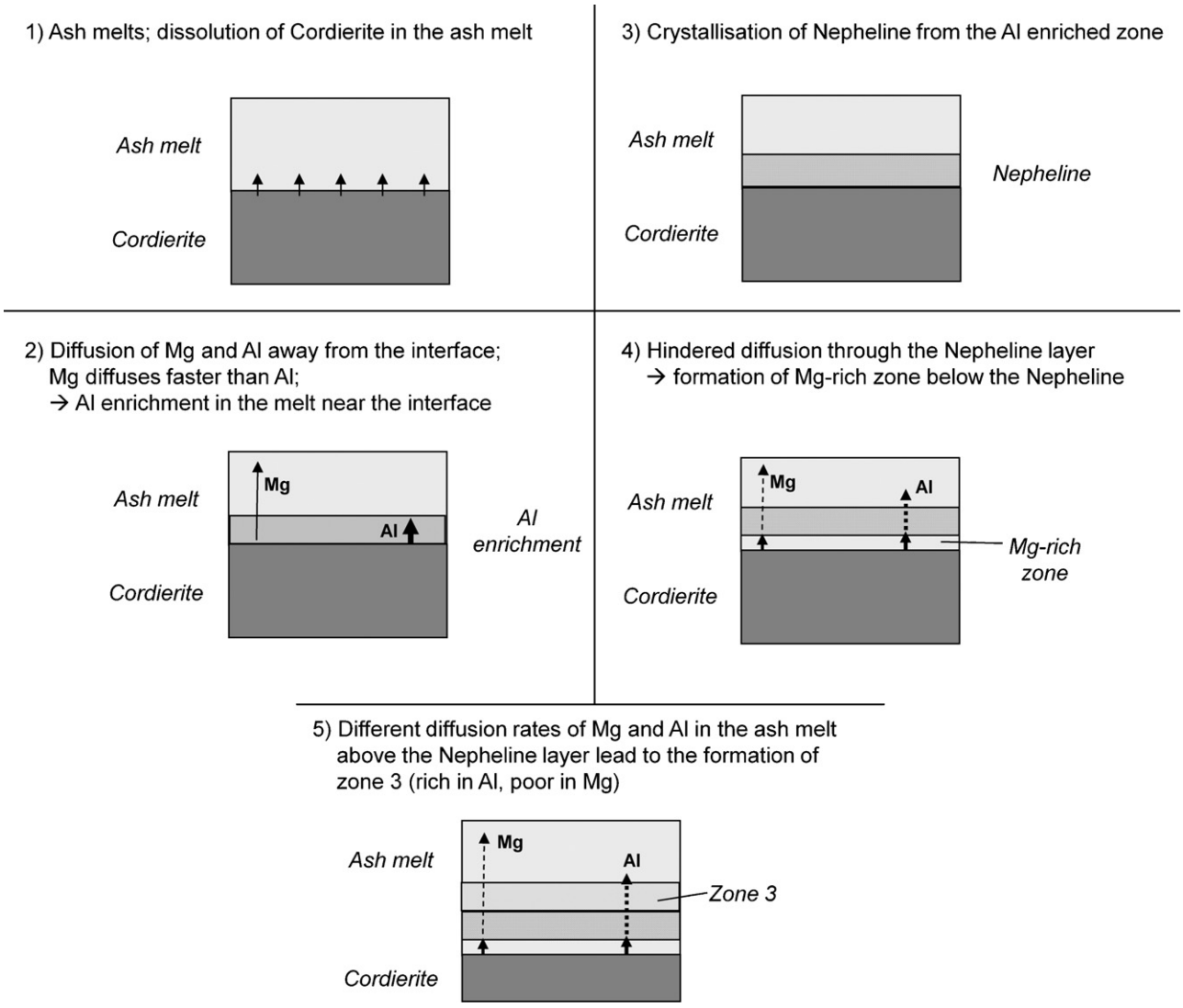

Fig. 10. Model for the attack of sodium silicate ash on Cordierite (cross-section).

of the Nepheline crystals. This causes the formation of the magnesium-rich zone 1 below the crystals observed in the samples treated at 1000 °C.

5. Above the Nepheline, the continued fast diffusion of Mg and the slow diffusion of Al in the ash melt lead to the formation of the alumina-rich and magnesia-poor zone 3. The continued development of such a profile will allow the Nepheline layer to grow slowly with time.

The model outlined above has therefore several stages: dissolution of Cordierite in the attacking melt, development of a compositional gradient, crystallization of a Nepheline barrier, causing a kinetic break and subsequent continued slower growth of a layered system. Even though an initial chemical reaction (dissolution) and kinetic breaks are involved, the process is mainly diffusion controlled. This explains the isotropy of the corrosion on a distinctly anisotropic material.

However, a diffusion rate limited model should – even with breaks – show a diminishing corrosion rate and ideally become parabolic at long times. The linear growth rate fitted for zone 1 (0.090 μm/min + 2.9 μm) in Fig. 5, which is equal to the recession of Cordierite during the corrosion process after the formation of the Nepheline layer, seems to contradict this model. We interpret this to be a mathematical problem:

According to the model, the recession rate of Cordierite, $dx_{\text{Cordierite}}/dt$, (the growth rate of zone 1) is proportional to the flux of Mg through the Nepheline layer which is defined as

$$D \cdot \frac{c_{\text{Mg,zone 1}} - c_{\text{Mg,zone 3}}}{x_{\text{Nepheline}}}$$

with D being the diffusion coefficient of Mg in the Nepheline layer, $c_{\text{Mg,zone 1}}$ and $c_{\text{Mg,zone 3}}$ being the Mg concentrations in zone 1 and 3 (below and above the Nepheline layer), respectively and $x_{\text{Nepheline}}$ being the thickness of the Nepheline layer. If the diffusion coefficient and the Mg concentrations below and above the Nepheline layer are constant as verified for the examined samples, the proportionality can be simplified to

$$dx_{\text{Cordierite}} \sim \frac{1}{x_{\text{Nepheline}}} dt.$$

Inserting the extrapolated growth rate for zone 2, i.e. the Nepheline layer, from Fig. 5 as $x_{\text{Nepheline}}$ (7.35 μm + 0.045 μm/min) and integrating gives

$$x_{\text{Cordierite}} \sim \frac{\ln(7.35 + 0.045 \cdot t)}{0.045}$$

for the time range between 0 and 60 min at 1000 °C with $x_{\text{Cordierite}}$ being the recession depth of Cordierite.

If this function is plotted for times between 0 and 60 min, only minor deviations from linearity occur. A linear extrapolation through the calculated data points has an R^2 value of 0.998. Such slight deviations from linearity cannot be visible from experimentally determined values for the thickness of zone 1 (i.e. the depth of Cordierite dissolved during the corrosion process) due to their scatter.

Therefore, the corrosion model developed above is in accordance with the measured data. The determined linear growth rate of zone 1 is a good approximation for the recession rate of Cordierite at 1000 °C after the barrier effect of the Nepheline layer (zone 2) has come into effect as long as extrapolations are not made for corrosion times ≫1 h.

4.2. Samples with phosphate ash

The absence of any reactions between Cordierite and ash at 1000 °C, where no indications for the melting of large portions of the ash were found, indicates that no significant corrosion via solid state reactions is occurring. At 1050 °C, strong melting of the ash occurs and excessive corrosion of the Cordierite substrate is evident. This suggests that melting of the ash is the decisive factor for the occurrence of significant corrosion.

The contents of Al and Si within the ash and the recession of the Cordierite surface below the ash after heat-treatments at 1050 °C show that the substrate is dissolved by the molten ash. The recession depth of the Cordierite is no reliable measure for the amount of corrosion due to its very irregular nature not allowing an exact quantification. A better measure for the amount of corrosion is the content of Al and Si within the reacted ash. The elements are not contained in the original ash and therefore give a measure of the amount of Cordierite dissolved in the ash during corrosion. The largely homogeneous distribution of the elements within the ash allowed a reasonable quantification by EDX. There were no significant differences in the Al or Si contents measured for samples with different orientations of ash relative to the Cordierite lattice (Fig. 9): the corrosion of Cordierite was equally strong for both orientations tested at 1050 °C.

There was no diffusion of ash elements into the Cordierite lattice detected, thus the corrosion by the phosphate ash is a surface process.

The following model (Fig. 11) was developed to explain the observed phenomena.

At 1000 °C, partial melting of the phosphate mixture is expected, because the lowest eutectic in the system $Ca_3(PO_4)_2$–$Zn_3(PO_4)_2$ lies at approximately 970 °C.[34] The melt is wetting grain boundaries within the ash and leads to liquid-phase assisted sintering; the capillary forces keep the small amounts of melt in the ash body and prevent significant attack of the Cordierite substrate. Between 1000 °C and 1050 °C, the melt formation from the ash becomes very strong. Due to the lack of a phase diagram for the system $Ca_3(PO_4)_2$–$Mg_3(PO_4)_2$–$Zn_3(PO_4)_2$, no exact information on the degree of melting is available. It is assumed that the major portion of the ash is molten at 1050 °C. This assumption is realistic, because a mixture of 50 mole% $Ca_3(PO_4)_2$ and 50 mole% $Zn_3(PO_4)_2$ would consist of approximately 80% melt at this temperature according to the phase diagram.[34] Further liquidus depression is likely in the ternary case with $Mg_3(PO_4)_2$ added.

The molten ash dissolves Cordierite quickly. The homogeneous distribution of Si and Al within the ash after the heat-treatments at 1050 °C indicates a fast diffusive distribution of the elements within the ash melt, i.e. very high diffusion rates for all elements involved are indicated for the phosphate melts.

There was no significant increase in the Al and Si contents of the ash measured after 20 min heat-treatment relative to the samples heat-treated for 10 min. We interpret this to be due to the fast diffusion: Within a short period of time (i.e. <10 min), the melt becomes saturated with Al and Si or at least reaches a state close to saturation. The amount of Cordierite dissolved becomes then a saturation limit controlled feature.

At high temperatures, Al and Si are in solution in the phosphate melt. The observed segregation takes place during cooling. Al and Si exsolve from the phosphate melt forming the grain-boundary phase dividing the phosphate within the ash into numerous small bodies. There is no information available from the experiments whether the segregated phase solidifies as an amorphous phase or whether it (partially) crystallizes during cooling. However, at least part of the Al and Si crystallize and form the silica and spinel phases identified within the reacted ash in addition to the grain-boundary phase.

The high concentrations of silica and zinc spinel inside and adjacent to cracks and the nearly complete transformation of Cordierite in the heat-treated powder mixture indicate that additional to the quick dissolution process, there is also a destruction of the Cordierite by reactions with the ash forming new crystalline phases. In the case of the ash-covered single crystals, this process is slow due to the limited area of contact between ash and Cordierite. The following type of reaction is assumed:

$$Mg_2Al_4Si_5O_{18} + 2CaMgZn(PO_4)_2 \text{ (in melt)}$$
$$\rightarrow\ 5SiO_2 + 2ZnAl_2O_4 + 2CaMg_2(PO4)_2 \text{ (in melt)}.$$

Here zinc from the phosphate melt reacts with the Cordierite to yield zinc-rich spinel and silica while magnesium is replacing the zinc in the phosphate melt. This reaction also explains why close to areas with high concentrations of silica and spinel, phosphates are often zinc-depleted.

Due to a lack of data for liquid $Zn_3(PO_4)_2$ or mixed orthophosphate melts, no thermodynamic calculation of the above reaction was possible. However, calculating the Gibb's

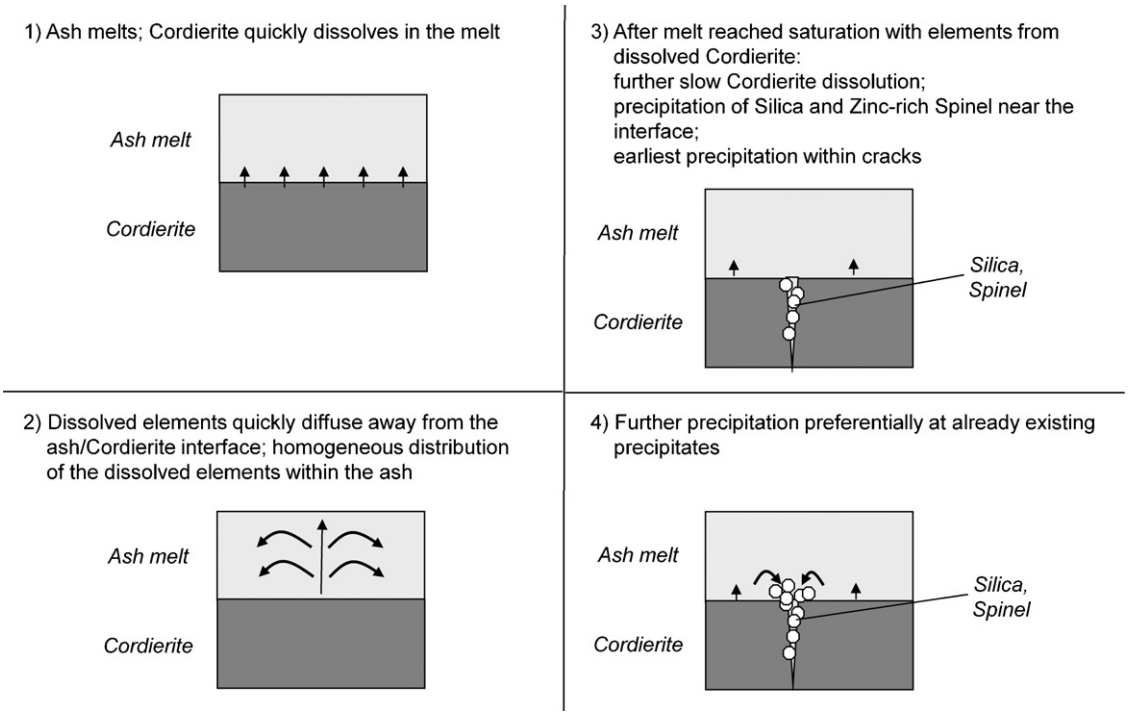

Fig. 11. Model for the attack of phosphate ash on Cordierite at 1050 °C (cross-section).

free enthalpy of the analogue reaction:

$$3Mg_2Al_4Si_5O_{18}\,(s) + 2Zn_3(PO_4)_2\,(s) \rightarrow 2Mg_3(PO_4)_2\,(s) + 6ZnAl_2O_4\,(s) + 15SiO_2\,(s)$$

with the software *FactSage*,[35] using data from[36] for zinc phosphate, gives a result of −208 kJ. Therefore the reaction is thermodynamically favorable and a comparable reaction of Cordierite with the zinc phosphate component of the ash melt seems likely.

It is assumed that the reaction process involves the steps:

(1) slow dissolution of Cordierite in the nominally saturated phosphate melt,
(2) over-saturation of the melt with elements from the Cordierite,
(3) crystallization of silica and spinel from the melt.

This process can explain why silica and spinel are locally clustered (especially within and adjacent to cracks) and do not form a continuous layer on the surface of the Cordierite. Inside melt-filled cracks, over-saturation of the phosphate melt can be more readily achieved than near the Cordierite surface due to the limited diffusion. The increased specific surface area of the crack compared to the normal Cordierite surface allows accelerated dissolution of the substrate by the melt. These mechanisms lead to an early precipitation of silica and spinel within the cracks. If nucleation of silica and spinel is limited within the melt and melt saturation has been reached, the elements dissolved from the Cordierite surface will diffuse to the sink, the already existing silica and spinel grains. This causes growth of the existing silica and spinel grains instead of formation of new crystals directly at the place where dissolution takes place.

It is important to note that the phosphate ash causes a remarkable amount of corrosion at 1050 °C – a temperature which is well within the range of temperatures possible during worst case DPF regenerations as published in the literature. The corrosion is clearly stronger than the corrosion caused by the sodium silicate melt at 1000 °C. In the literature, especially alkaline compounds have been emphasized as critical in terms of a possible corrosive attack on Cordierite.[6,8,12,15,17–20,28] It has been reported that phosphorous-rich ashes may form melts at temperatures above approximately 1000 °C[4,5] and react with Cordierite at temperatures above 1100 °C,[37] but the large amount and high rate of Cordierite corrosion by phosphate melts at temperatures below 1100 °C (especially in the early stage when the substrate is dissolved in the phosphate melt) have not yet been reported. This corrosion process may be of great importance for the degradation of Cordierite DPF as phosphates of Ca, Mg and Zn are contained in many ashes in high amounts.[3,9–11]

Unambiguous statements on possible differences in the corrosion rates along different directions of the Cordierite lattice cannot be deduced from the experiments made. According to the corrosion model explained above, the dissolution of Cordierite in the ash melt is largely finished in less than 10 min at 1050 °C. Therefore, the likely difference in the dissolution rate for different orientations of the Cordierite lattice does not play any role for the result, because the saturation limit is reached in each case in the experiments with 10 and 20 min dwell time at 1050 °C. The (slower) secondary corrosion process by reactions between Cordierite and melt leading to the formation of silica and spinel could not be reasonably quantified due to the

irregular and inhomogeneous distribution of the reaction products.

5. Summary and conclusions

Silica- and sodium-rich melts as they might originate from reactions between alkali ash compounds and Cordierite or by reactions between silica and alkali compounds within ashes attack Cordierite at 900 °C and 1000 °C by dissolving it. By diffusion processes, compositional gradients develop, which lead eventually to the formation of several layers with different compositions, including a crystalline Nepheline layer which acts as a diffusion barrier. The exact corrosion mechanism in the very early stage of ash attack on the Cordierite remains to be determined. Further experiments at temperatures below 1000 °C and/or with short dwell times would be necessary to gather more information on the ash attack under such conditions.

In the later stage of the corrosion process (after the formation of a Nepheline layer), Cordierite is dissolved in a process controlled by the diffusion of magnesium through the Nepheline layer into the ash. Due to the short observation time of the growth of the Nepheline layer, the corrosion rate at 1000 °C for times up to 1 h is well approximated by a linear rate of 0.09 μm/min.

Many literature reports have stressed the high potential of alkali compounds for corrosively damaging Cordierite DPF. Corrosion temperatures several hundred degrees below 1000 °C are known from the reports cited in Section 1. However, as mentioned in Section 2, many ashes from DPF contain only low amounts of alkalis according to literature,[3,9,11,32] so the importance of alkali corrosion for the degradation of DPF in the field might be lower than expected in earlier years. Additionally, if reactions between Cordierite and alkali compounds cause melt formation, as it is known from literature reports,[17,18] a corrosion behavior similar to the sodium silicate ash studied here has to be expected, which tends to slow down by a diffusion barrier formation.

Nonetheless, if a DPF collects high amounts of alkaline compounds from sources as mentioned in Section 1 or if molten alkaline compounds segregate from an ash and are concentrated on a filter surface, we still may see a significant damage from this type of attack. Also, the observed damage mechanism is relevant in the consideration of Cordierite in special combustion environments, which are known to cause problems of hot corrosion.

No dependence of the corrosion process or rate on the orientation of ash relative to the Cordierite lattice was observed. This is due to the fact that the corrosion process is diffusion controlled.

In accordance with earlier findings by Bachiorrini,[28] no diffusion of sodium into the Cordierite lattice is occurring during the corrosion process according to measurements by EDX and TOF-SIMS. This is also true for the diffusion of other elements from the experiments in the phosphate ash system.

The phosphate ash did not attack Cordierite substrates at 1000 °C, but strong corrosion was observed at 1050 °C in connection with a strong melting of the ash. The corrosion process shows two stages. During the first stage, Cordierite is dissolved in the molten ash; dissolved elements are quickly distributed within the ash melt by diffusion. This first stage of corrosion is proceeding quickly. In the experimental setup used, it was terminated in less than 10 min at 1050 °C. The second stage of corrosion destroys Cordierite by the formation of spinel and silica upon the reaction between the ash melt (or, more precisely, the zinc phosphate component of the ash melt) and the substrate. In the experiments performed on single crystals of Cordierite, this second process proceeded slowly due to the low surface area of the substrates. In particulate filters, however, the process may proceed at a much higher rate due to the large surface area of the porous filter material (especially when molten ash infiltrates the pore structure) and thus contribute strongly to filter deterioration. A kinetic law for the corrosion rate could not be determined due to the fast rate of the first stage (dissolution of Cordierite) and problems encountered in quantifying the second stage (formation of spinel and silica) of the process. Further experiments will be necessary to determine the rates and the possible orientation dependence of the two stages of corrosion by the phosphate ash.

The corrosion process in the presence of the phosphate ash is of high relevance for the potential corrosion of DPF in the field. Phosphates of Ca, Mg and Zn are main constituents in many ashes found in DPF according to literature[3,9–11] and are strikingly aggressive once they form a melt.

Acknowledgements

The authors would like to thank Dr. Christoph Berthold (University of Tübingen, Applied Mineralogy), Dr. Christiane Müller and Dr. Thomas Köhler (Robert Bosch GmbH, CR/ARA) who conducted the XRD measurements discussed in this paper as well as Dr. Herbert Feld and Dr. Markus Deimel (OFG Analytik GmbH) who conducted the TOF-SIMS measurements. Furthermore, the authors would like to thank the German *Bundesministerium für Bildung und Forschung* for financial support (Project *CorTRePa*, promotional reference 03X3502).

References

1. Rasch H. Considering some thermal applications for cordierite and cordierite–mullite materials. *Berichte der DKG* 1987;(11/12): 454–8.
2. Lachmann IM, Bagley RD, Lewis RM. Thermal expansion of extruded cordierite ceramics. *JACS Bulletin* 1981;**60**(2):202–5.
3. Merkel GA, Cutler WA, Warren CJ. *Thermal durability of wall-flow ceramic diesel particulate filters*; 2001. SAE Special Publication [SP-15829-23].
4. O'Sullivan D, Hampshire S, Pomeroy MJ, Murtagh MJ. Comparison of corrosion resistance of cordierite and silicon carbide diesel particulate filters to combustion products of diesel fuel containing Fe and Ce additives. *Ceramic Engineering and Science Proceedings* 2004;**25**(3): 415–20.
5. O'Sullivan D, Pomeroy MJ, Hampshire S, Murtagh MJ. Degradation resistance of silicon carbide diesel particulate filters to diesel fuel ash deposits. *Journal of Materials Research* 2004;**19**(10):2913–21.
6. Agostini L, Borello C, Demaestri PP, Giachello A, De Portu G, Giucciardi S. Effects of sodium and iron on the thermomechanical properties of porous cordierite traps for diesel engines. Presentation at European Ceramic Society 2nd conference; 1991.

7. Frank RW, Hardenberg HO. Reduction of particulate emission from the break-in facilities of a heavy-duty engine plant by means of ceramic monolith traps. SAE-Paper 850268; 1985. p. 1–10.
8. Scardi P, Sartori N, Giachello A, Demaestri PP, Branda F. Influence of calcium oxide and sodium oxide on the microstructure of cordierite catalyst supports. *Ceramics International* 1993:19105–11.
9. Barris MA, Reinhart SB, Wahlquist FH. The influence of lubricating oil and diesel fuel ash accumulation in an exhaust particulate trap. SAE-Paper 910131; 1991. p. 19–28.
10. Tsuchihashi K, Shirakawa H, Saitoh Y. Experimental analysis for accumulated ash in DPF—effect of high quality low ash oil. *Review of Automotive Engineering* 2004;**25**:285–9.
11. Givens WA, Buck WH, Jackson A, Kaldor A, Hertzberg A, Moehrmann W, et al. Lube formulation effects on transfer of elements to exhaust aftertreatment system components. SAE-Paper 2003-01-3109; 2003. p. 1–15.
12. Montanaro L, Bachiorrini A. Influence of some pollutants on the durability of cordierite filters for diesel cars. *Ceramics International* 1994;**20**:169–74.
13. Rose D, Boger T. Diesel particulate filter durability for Euro 5 and future Euro 6 applications. Presentation at 4th international CTI forum "diesel particulate filter", Frankfurt; 2007.
14. Hickman DL, Ebener S, Zink U. Reduction of particulate emissions from diesel passenger cars and heavy duty vehicles. *Fortschritt-Berichte VDI-Reihe 12: Verkehrstechnik/Fahrzeugtechnik*, vol. 455. VDI-Verlag; 2001. p. 267–285.
15. von Watzdorf HV. Korrosionsbeständigkeit offenporöser Cordierit-Wabenkörper in natriumadditivierten dieselmotorischen Abgasen. PhD/Doctoral thesis. RWTH, Aachen; 1996.
16. Scardi P, Sartori N, Giachello A, Demaestri PP, Branda F. Thermal stability of cordierite catalyst supports contaminated by Fe_2O_3, ZnO and V_2O_5. *Journal of the European Ceramic Society* 1994;**13**:275–82.
17. Montanaro L, Negro A. On the effects induced by the accumulation of sodium, iron and cerium, on diesel soot filters. SAE Technical Paper 980540; 1998. p. 139–147.
18. Montanaro L. Durability of ceramic filters in the presence of some diesel soot oxidation additives. *Ceramics International* 1999;**25**: 437–45.
19. Negro A, Montanaro L, Demaestri PP, Bachiorrini A. Interaction between some oxides and cordierite. *Journal of the European Ceramic Society* 1993;**12**:493–8.
20. Montanaro L, Bachiorrini A, Negro A. Deterioration of cordierite honeycomb structure for diesel emissions control. *Journal of the European Ceramic Society* 1994;**13**:129–34.
21. Cutler WA, Merkel GA. A new high temperature ceramic material for diesel particulate filter applications. SAE-Paper 2000-01-2844; 2000. p. 79–87.
22. Yamanaka M, Okazaki Y. Hot-corrosion resistance of Fe–Cr–Al substrate to alkali metals for NOx adsorption. In: Bode, editor. *Metal-supported automotive catalytic converters*. Frankfurt: H. Werkstoff-Informationsgesellschaft mbH; 1997. p. 127–35.
23. Choi B, Kang H, Son G, Hwang C. Thermal aging behavior of SiC substrate in the presence of ash materials and alkali metals. SAE-Paper 2007-01-1939; 2007. p. 1031–1037.
24. Krutzsch B, Wenninger G, Lindner E, Pabel M. Diesel fuel containing an additive which improves the combustion of soot. United States Patent 5522905; 4 June 1996.
25. Fischer J. Biodiesel und Abgasnachbehandlung. Presentation at 3 FAD-Konferenz "Herausforderung Abgasnachbehandlung für Dieselmotoren", Dresden; 2005.
26. Winterstein G, Mürbe J, Tupaika F. Polymorphie von Cordierit in natürlichen Mineralien und in Cordieritwerkstoffen. *Keramische Zeitschrift* 2003;**55**(3):160–5.
27. Sorrell CA. Reaction sequence and structural changes in cordierite refractories. *Journal of the American Ceramic Society* 1960;**43**(7):343–87.
28. Bachiorrini A. New hypotheses on the mechanism of the deterioration of cordierite diesel filters in the presence of metal oxides. *Ceramics International* 1996:2273–7.
29. Fox DS, Jacobson NS. Molten-salt corrosion of silicon nitride. I. Sodium carbonate. *Journal of the American Ceramic Society* 1988;**71**(2):128–38.
30. Jacobson NS. Kinetics and mechanism of corrosion of SiC by molten salts. *Journal of the American Ceramic Society* 1986;**69**(1):74–82.
31. Levin EM, McMurdie HF, Hall FP. *Phase diagrams for ceramists*. Columbus, OH: The American Ceramic Society; 1956.
32. Kimura K, Lynskey M, Corrigan ER, Hickman DL, Wang J, Fang HL, et al. Real world study of diesel particulate filter ash accumulation in heavy-duty diesel trucks. SAE-Paper 2006-01-3257; 2006. p. 1–31.
33. Christou SY, Birgersson H, Efstathiou AM. Reactivation of severely aged commercial three-way catalysts by washing with weak EDTA and oxalic acid solutions. *Applied Catalysis B: Environmental* 2007;**71**:185–98.
34. Levin EM, Robbins CR, McMurdie HF. *Phase diagrams for ceramists—1969 supplement*. Columbus, OH: The American Ceramic Society; 1969.
35. Bale CW, Chartrand P, Degterov SA, Eriksson G, Hack K, Ben Mahfoud R, et al. FactSage thermochemical software and databases. *Calphad* 2002;**26**(2):189–228.
36. Barin I. *Thermochemical data of pure substances*. Weinheim: VCH Verlagsgesellschaft mbH; 1993.
37. O'Sullivan D, Hampshire S, Pomeroy MJ, Fordham RJ, Murtagh J. Resistance of cordierite diesel particulate filters to corrosion by combustion products of diesel fuel containing ferrocene. Presentation at ISATA, Dublin; 2000.